Selected papers presented at the Eleventh Annual Conference of the Materials Research Society of Serbia, YUCOMAT 2009

Electrochemical Behaviour of V_2O_5 Xerogel and V_2O_5 Xerogel/C Composite in an Aqueous $LiNO_3$ and $Mg(NO_3)_2$ Solutions

I. Stojković[a,*], N. Cvjetićanin[a], S. Marković[b], M. Mitrić[c] and S. Mentus[a]

[a]University of Belgrade, Faculty of Physical Chemistry, Studentski Trg 12-16, 11158 Belgrade, Serbia

[b]Institute of Technical Sciences of the Serbian Academy of Sciences and Arts, Knez Mihailova 35/IV, 11001 Belgrade, Serbia

[c]The Vinča Institute, Condensed Matter Physics Laboratory, P.O. Box 522, 11001 Belgrade, Serbia

We synthesized both the V_2O_5 xerogel and the composite V_2O_5 xerogel/C starting from the solution of V_2O_5 in hydrogen peroxide. After the characterization by XRD, thermal (TGA-DTA), SEM methods and by particle size analysis, the investigation of Li^+ and Mg^{2+} intercalation/deintercalation reactions in an aqueous solutions of $LiNO_3$ and $Mg(NO_3)_2$ were performed by cyclic voltammetry. The composite material V_2O_5 xerogel/C displayed relatively high intercalation capacity, amounting to 123 mA h g^{-1} and 107 mA h g^{-1}, in lithium and magnesium salt solutions, respectively.

PACS numbers: 82.47.Aa, 71.20.Tx, 82.45.Yz, 82.80.Fk, 65.40.gk

1. Introduction

The crystalline materials of layered structure, such as $LiCoO_2$, $LiMn_2O_4$, V_2O_5, $Li_{1+x}V_3O_8$, known as capable of formation of intercalate compound with lithium, were frequently used as electrode materials in Li-ion batteries. Many literature reports about the Li-intercalation reactions relate preferably to the non-aqueous solutions. Quite recently, several studies appeared aimed to the intercalation in aqueous solutions [1–4]. A magnesium-ion rechargeable battery might be very attractive, too. For instance, some authors reported that vanadium bronzes [5, 6], graphite fluorides [7] and transition metals oxides [6, 8, 9] may intercalate magnesium, and thus they may be considered as electrode materials for secondary Mg-ion batteries. However, on the present level of knowledge, such a type of battery suffers of two unresolved problems, the first one being the passivation of metallic magnesium if used as anode in commonly used organic electrolytes, and the second one being low capacity utilization during the Mg-intercalation process [10, 11].

Crystalline V_2O_5 is capable of electrochemical intercalation of Li^+ and Mg^{2+} ions in organic electrolytes, with relatively fair cycling performance [6, 8, 12]. The amorphous, hydrated form of vanadium pentoxide (V_2O_5 nH_2O), has a higher intercalation capacity than its crystalline form, and this was explained by the fact that water molecules expend the interlayer distance of this compound [13]. Under cathodic polarization, the V_2O_5 nH_2O xerogel can insert up to three Li atoms, while orthorhombic V_2O_5 can insert only one Li ion [13]. Xerogel V_2O_5 nH_2O can be prepared by the dissolution of V_2O_5 in an aqueous hydrogen peroxide solution [14, 15] following by solvent evaporation. By an analogous procedure enlarged by addition of acetylene black, composite V_2O_5/C can be synthesised. There exist the literature data that in organic electrolyte solutions, both lithium and manganese ions may be reversibly intercalated into V_2O_5/C composite at an acceptably high rate [11, 16, 17]. However, similar examinations in aqueous solutions were not published thus far.

In the present work, we synthesized both pure V_2O_5 xerogel and its composite with carbon black, starting from the aqueous solution of V_2O_5 in hydrogen peroxide. The intercalation reactions of Li^+ and Mg^{2+} ions in these materials were studied in aqueous solutions of $LiNO_3$ and $Mg(NO_3)_2$ by means of cyclic voltammetry.

2. Experimental

2.1. Sample preparation

A Merck p.a. crystalline V_2O_5 (1 g) was added to 100 ml of 10% H_2O_2 solution in a glass vessel. In a short time, V_2O_5 was completely dissolved yielding the clear yellow solution. To one half of this solution, carbon black (Vulcan®, Cabot Corp., particle diameter about 30 nm) was added in an amount of 10 wt.% relative to V_2O_5. This suspension was then stirred in a glass vessel by a magnetic stirrer for 24 h. After several days spent in free air at room temperature, the majority of the solvent evaporated from both solutions, leaving the powdered precursors. In order to finalize the active electrode

* corresponding author; e-mail: ivana@ffh.bg.ac.rs

materials, the simple V_2O_5 xerogel and the V_2O_5/C xerogel composite, these precursors were additionally dried at 200 °C for one hour.

2.2. Methods of sample characterization

The morphology of the samples was observed by the scanning electron microscope (SEM) JEOL JSM-6460 LV. The particle size distribution was determined by means of the particle size analyzer Mastersizer 2000, Malvern Instruments.

Simultaneous thermogravimetry/differential thermal analysis (TGA/DTA) in the temperature range 25 to 550 °C was carried out in the air atmosphere, at a heating rate of 10 °C min^{-1} using the thermobalance TA SDT, Model 2960.

The X-ray diffractometry on powder (XRPD) was carried out in a transmission mode, using the Bruker D8 Advance diffractometer and the CuK$\alpha_{1,2}$ radiations source. For fast structure analysis, the 10–70° 2θ range was used, with the 0.05° step, and two seconds exposition time.

2.3. Electrode preparation and electrochemical measurements

The samples of active electrode materials, synthesized as described in the Sect. 2.1, were used to compose the working electrodes aimed for electrochemical investigations. The working electrodes were prepared in the following way: 60 wt.% of the active powder, 30 wt.% carbon black and 10 wt.% of poly (vinylidene fluoride) (PVDF) binder were added together to a *N*-methyl-2--pyrrolidone solvent. This slurry was homogenised for 1 h in an ultrasonic bath, and one drop was taken and spread over a glassy carbon stick, which was then heated under vacuum at 140 °C for about 4 h to evaporate solvent. Apart of working electrode, a classical three-electrode cell arrangement involved also wide platinum foil as a counter electrode, and a saturated calomel electrode (SCE) as a reference electrode. The aqueous $LiNO_3$ and $Mg(NO_3)_2$ solutions (the last one being purchased in a form of hexahydrate) were used as electrolytes. The cell was connected to a potentiostat/galvanostat Gamry PCI4/300. The cyclovoltammograms were recorded at a scan rate of 10 mV s^{-1}. The potential limits used for cyclic voltammetry were −1 V and +1 V with respect to (SCE), dictated by the onset of evolution of hydrogen and oxygen, respectively. The coulombic capacity was calculated on the basis of the surface under the voltammetric curves.

3. Results and discussion

3.1. Structure and morphology

The precursors obtained by spontaneous drying of both V_2O_5 + H_2O_2 and V_2O_5 + H_2O_2 + C solutions at a room temperature were subjected to TGA in order to determine the percentage of residual water. The heating up to 200 °C, as Fig. 1 shows, causes the deliberation of roughly 13 wt.% of water, which corresponds to 1.6 moles of water per one mole of V_2O_5. This presents almost complete content of residual water, since the main mass loss related to the water deliberation finishes at roughly 150 °C. Thus, the procedure of preparation of active electrode material (Sect. 2.1) involved the drying of the precursors at 200 °C. The heating of composite V_2O_5 + H_2O_2 + C above 300 °C caused the combustion of C, accompanied by an intense exothermic peak of the DTA curve. The mass loss caused by combustion corresponds to the initial content of C in the composite.

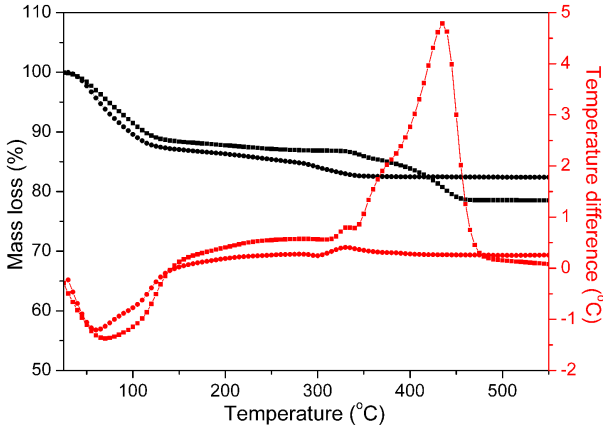

Fig. 1. The TG (black symbols) and DTA (red symbols) curves of the products obtained by spontaneous drying at room temperature of the solutions of (•) V_2O_5 and (■) V_2O_5 + 10 wt.% C in hydrogen peroxide. The heating rate used to record the thermograms was 10 °C min^{-1}.

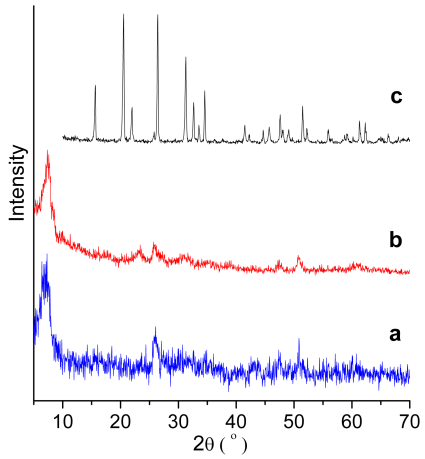

Fig. 2. The X-ray diffraction pattern of (a) xerogel V_2O_5, (b) the V_2O_5 xerogel/C composite, and (c) the product obtained by heating of xerogel V_2O_5 to 330 °C.

The products obtained upon drying at 200 °C, both pure and composite xerogel samples, retained an amorphous structure, as evidenced by the X-ray diffractograms shown in Fig. 2a and b. An analogous amorphous structure was evidenced by Wang et al. [13] upon

drying the solution of V_2O_5 in H_2O_2, as well as by quenching of molten V_2O_5 [18]. This stage of material we call xerogel, since such a term was already used elsewhere [13, 19, 20].

The TGA curve of pure V_2O_5 xerogel shows the termination of any mass loss for temperatures higher than 327 ℃. The XRD analysis of a pure xerogel sample heated previously to 330 ℃ (Fig. 2c) evidenced the crystalline structure, corresponding to V_2O_5 of orthogonal symmetry (JCPDS card No 41-1426) [13]. In the case of composite sample, the combustion of carbon, which started somewhat above 327 ℃, caused that the mass of the sample became temperature independent just beyond 450 ℃. However, in analogy to the pure xerogel sample, for a composite sample, we may account with the amorphous-to-crystalline transition at 327 ℃, too.

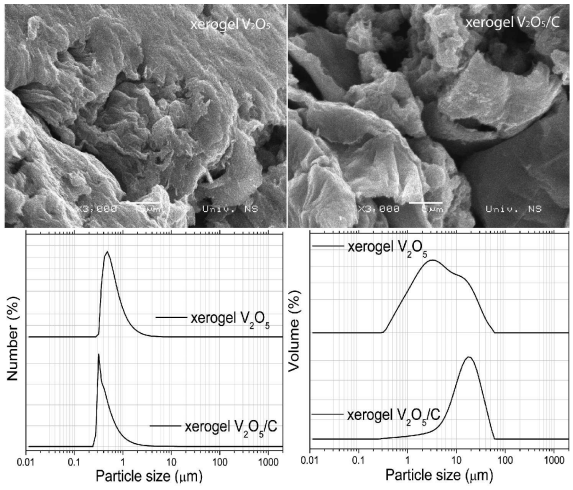

Fig. 3. The SEM microphotographs (top) and the number and volume against particle diameter distribution curves of xerogel V_2O_5 and V_2O_5 xerogel/C composite.

The SEM images of the samples are presented in Fig. 3. Both sample types show flaky appearance, with smaller flakes for the composite sample. The particle size distribution was determined in an isopropanol suspension, according to the manufacturer's manual. The particle diameter of pure V_2O_5 xerogel is centered around 540 nm. The particle diameter of composite V_2O_5 xerogel/C sample show narrower distribution around the mean value of 400 nm. The particles bearing the majority of the volume of the sample are centered around to 5 and 12 μm for pure and composite xerogel sample, respectively. This analysis indicated the structureless V_2O_5 flakes, in which, for the composite case, very fine C particles (invisible at the actual magnification) are embedded.

3.2. Electrochemical properties

The electrochemical performance of the samples was tested in saturated aqueous solutions of both $LiNO_3$ and $Mg(NO_3)_2$, by cyclic voltammetry method. The series of cyclovoltammograms recorded at a common scan rate was 10 mV s^{-1} is presented in Fig. 4. The current axis unity is amper per gram, being practical for coulombic capacity calculation. The voltammograms indicate preferably two stage intercalation/deintercalation processes. The positions of cathodic peaks for the xerogel V_2O_5/C composite in $LiNO_3$ are −0.25 and 0.56 V vs. SCE while the positions of anodic peaks are −0.37, 0.23 and 0.69 V vs. SCE, which is similar to the peak positions found elsewhere [13]. In saturated aqueous solution of $Mg(NO_3)_2$, cathodic peaks occur at 0.25 and −0.25 vs. SCE, while corresponding anodic peaks occur at −0.1 and 0.63 V vs. SCE. The peaks of composite samples are always much higher than the peaks of pure xerogel V_2O_5 (compare the spread of the left and the right current axes). The intercalation/deintercalation reactions of both Li^+ and Mg^{2+} ions are obviously much faster in the case of V_2O_5 xerogel/C composite than in the case of pure V_2O_5 xerogel.

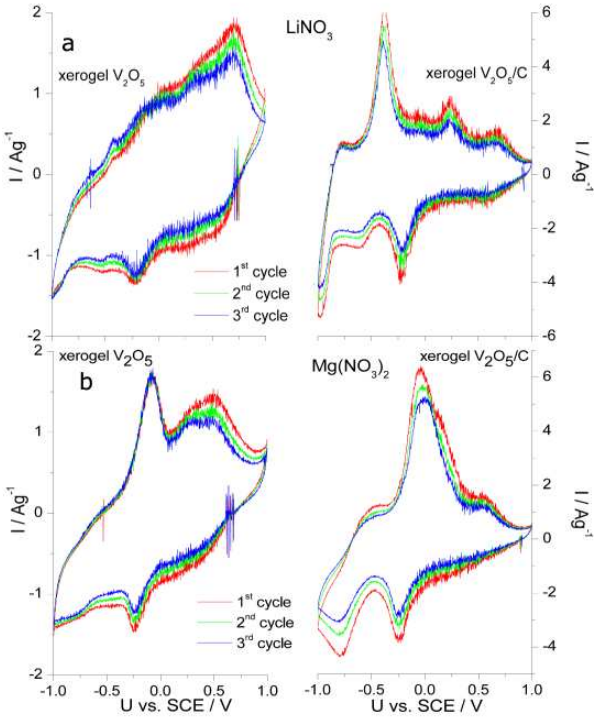

Fig. 4. The cyclovoltammetric curves of xerogel V_2O_5 (left) and V_2O_5 (right) xerogel/C composite in saturated solution of (a) $LiNO_3$ and (b) $Mg(NO_3)_2$. The scan rate was 10 mV s^{-1}.

The coulombic capacities were calculated from the surfaces of the cathodic and anodic parts of the cyclovoltammograms. In the Li-salt solution, the pure xerogel V_2O_5, with the coulombic capacity of 50 mA h g^{-1}, offered no any advantage in relation to crystalline V_2O_5 which, according to our previous study [21], yielded 63 mA h g^{-1}. Similar relations hold for Mg-salt solution, in which xerogel V_2O_5 yielded 50 mA h g^{-1} while crystalline V_2O_5 yielded 30 mA h g^{-1} [21]. However, V_2O_5 xerogel/C

composite, yielded 123 mA h g^{-1} in $LiNO_3$ solution and 107 mA h g^{-1} in $Mg(NO_3)_2$ solution.

In view of the fact that V_2O_5 is an insulating compound from the standpoint of battery action, the role of carbon black addition is to improve the utilization of coulombic capacity of V_2O_5. To both of the electrode materials a lot of carbon black (30%) was added during electrode preparation. Obviously, a much smaller addition (10%) of carbon black during the V_2O_5 xerogel/C composite synthesis enabled a substantially improved electrochemical behaviour of this electrode material in aqueous solution of Li and Mg salts. This may be explained closer electrical contact between V_2O_5 xerogel and carbon particles [17], which was achieved during the evaporation of V_2O_5 solution in the presence of carbon black.

4. Conclusions

The V_2O_5 xerogel and the V_2O_5 xerogel/C composite were obtained by dissolution of crystalline V_2O_5 in 10 wt.% H_2O_2 and water evaporation at room temperature, in both the absence and the presence of 10 wt.% of carbon black. After drying at 200 ℃, both these materials were used to made electrodes, which were examined by cyclic voltammetry in aqueous the solutions of lithium and magnesium nitrates. The intercalation/deintercalation reactions, involving Li and Mg ions, enabled the coulombic capacity, amounting to 123 mA h g^{-1} and 107 mA h g^{-1} in $LiNO_3$ and $Mg(NO_3)_2$ aqueous solutions, respectively, for V_2O_5 xerogel/C composite, which is acceptable from the viewpoint of commercial use. Simple V_2O_5 xerogel did not display so high capacity, and this fact was explained in view of the quality of electrical contact achieved during the production of the electrode material.

Acknowledgments

This work was supported by the Ministry of Science and Technological Development of Republic Serbia, Project No. 142047.

References

[1] L. Tian, A. Yuan, *J. Power Sources* **192**, 693 (2009).

[2] N. Cvjeticanin, I. Stojkovic, M. Mitric, S. Mentus, *J. Power Sources* **174**, 1117 (2007).

[3] R. Ruffo, C. Wessells, R.A. Huggins, Y. Cui, *Electroch. Commun.* **11**, 247 (2009).

[4] X. Cao, L. Xie, H. Zhan, Y. Zhou, *Mat. Res. Bull.* **44**, 472 (2009).

[5] P. Novak, W. Scheifele, F. Joho, O. Haas, *J. Electrochem. Soc.* **142**, 2544 (1995).

[6] P. Novák, R. Imhof, O. Haas, *Electrochim. Acta* **45**, 351 (1999).

[7] J. Giraudet, D. Claves, K. Gu'erin, M. Dubois, *J. Power Sources* **173**, 592 (2007).

[8] L. Yu, X. Zhang, *J. Colloid Interface Sci.* **278**, 160 (2004).

[9] M.E. Spahr, P. Novák, O. Haas, R. Nesper, *J. Power Sources* **54**, 346 (1995).

[10] L. Jiao, H. Yuan, Y. Wang, J. Cao, Y. Wang, *Electroch. Commun.* **7**, 431 (2005).

[11] D. Imamura, M. Miyayama, M. Hibino, T. Kudo, *J. Electrochem. Soc.* **150**, A753 (2003).

[12] G.G. Amatucci, F. Badway, A. Singhal, B. Beaudoin, G. Skandan, T. Bowmer, I. Plitz, N. Pereira, T. Chapman, R. Jaworskia, *J. Electrochem. Soc.* **148**, A940 (2001).

[13] Y. Wang, H. Shang, T. Chou, G. Cao, *J. Phys. Chem. B* **109**, 11361 (2005).

[14] B. Alonso, J. Livage, *J. Solid State Chem.* **148**, 16 (1999).

[15] C. Fontenot, J.W. Wiench, M. Pruski, G.L. Schrader, *J. Phys. Chem. B* **104**, 11622 (2000).

[16] D. Imamura, M. Miyayama, *Solid State Ionics* **161**, 173 (2003).

[17] T. Kudo, Y. Ikeda, T. Watanabe, M. Hibino, M. Miyayama, H. Abe, K. Kajita, *Solid State Ionics* **152-153**, 833 (2002).

[18] S.H. Ng, S.Y. Chew, J. Wang, D. Wexler, Y. Tournayre, K. Konstantinov, H.K. Liu, *J. Power Sources* **174**, 1032 (2007).

[19] I. Stojković, N. Cvjetićanin, I. Pašti, M. Mitrić, S. Mentus, *Electroch. Commun.* **11**, 1512 (2009).

[20] L.M. Chen, Q.Y. Lai, Y.J. Hao, Y. Zhaoa, X.Y. Ji, *J. Alloys Comp.* **467**, 465 (2009).

[21] I. Stojković, I. Pašti, N. Cvijetićanin, M. Mitrić, S. Mentus, *Proceedings of the 9th International Conference on Fundamental and Applied Aspects of Physical Chemistry, Belgrade*, 279 (2008).